

Research paper

Stress Wave Tomogram and Wood Density Profile in a Royal Palm Tree: a Case Study

Yue-Hsing Huang,¹⁾ Chih-Hsin Chung,²⁾ Meng-Ling Wu,³⁾ Cheng-Jung Lin^{4,5)}

【 Summary 】

This study examined transverse stress wave tomographies and wood density (D) profiles of a royal palm (*Roystonea regis*) tree trunk at different heights. Moreover, effects of different moisture contents (MCs of 60~270%) on the transverse stress wave velocity (V) during desorption were investigated. Results showed that the highest V and D values on the tree trunk were both located in the peripheral region at 2 m above the ground, while the lowest V and D values on the tree trunk were found in the inner region at 5~6 m above the ground. Corresponding radial V values of the undamaged disc cross-section from the peripheral region to the inner region showed a symmetrical layered structure. Visual inspection of disc cross-section revealed a larger thickness and ratio of the peripheral region in the tree trunk at the tree base. The relationship between the D (at about 12% MC) and V (green) can be expressed by a second-order polynomial regression ($R^2 = 0.82, p < 0.01$). The V was significantly ($R^2 = 0.61, p < 0.01$) affected by the MC and tended to increase with an increasing MC. When making an acoustic inspection, it is necessary to adjust the V of standing trees with different MCs for comparison purposes and to achieve higher accuracy, which would in turn yield more-accurate tree inspection assessments.

Key words: evaluation of hazardous trees, tomogram, stress wave, tree risk assessment, wood density profile.

Huang YH, Chung CH, Wu ML, Lin CJ. 2013. Stress wave tomogram and wood density profile in a royal palm tree: a case study. *Taiwan J For Sci* 28(3):129-44.

¹⁾ Director General, Taiwan Forestry Research Institute, 53 Nanhai Rd., Taipei 10066, Taiwan. 林業試驗所所長室, 10066台北市南海路53號。

²⁾ Department of Forest Management, Taiwan Forestry Research Institute, 53 Nanhai Rd., Taipei 10066, Taiwan. 林業試驗所森林經營組, 10066台北市南海路53號。

³⁾ Department of Forest Protection, Taiwan Forestry Research Institute, 53 Nanhai Rd., Taipei 10066, Taiwan. 林業試驗所森林保護組, 10066台北市南海路53號。

⁴⁾ Department of Forest Utilization, Taiwan Forestry Research Institute, 53 Nanhai Rd., Taipei 10066, Taiwan. 林業試驗所森林利用組, 10066台北市南海路53號。

⁵⁾ Corresponding author, e-mail:d88625002@yahoo.com.tw 通訊作者。

Received May 2013, Accepted August 2013. 2013年5月送審 2013年8月通過。

研究報告

大王椰子的應力波斷層影像及木材密度圖譜檢測之 案例報告

黃裕星¹⁾ 鍾智昕²⁾ 吳孟玲³⁾ 林振榮^{4,5)}

摘要

本研究檢測大王椰子樹在不同高度的樹幹應力波斷層影像及木材密度(D)圖譜，並調查水分在脫濕過程中不同含水率(MC = 60~270%)對橫向應力波速度(V)的影響。結果發現樹幹橫斷面中，最高V及D是位於外圍周邊區域(外殼厚度)及樹高2公尺位置，最低V及D是位於中央區域及樹高5~6公尺位置。未損壞樹幹橫斷面從外殼區域到中央區域的相對應橫向V圖譜，在橫斷面上形成一個對稱的層狀結構圖。目視檢查發現樹木基部之樹幹橫斷面有較大的外殼厚度及比例。D(MC約12%)與V(生材狀況)之間的關係可用一元二次複迴歸表達(決定係數， $R^2 = 0.82$, $p < 0.01$)。實際檢測樹幹橫斷面時，MC愈高時V愈高，MC顯著的影響V值($R^2 = 0.61$, $p < 0.01$)。因此，當在現場檢測大王椰子立木時，可以依據不同的MC來調整獲得更精確的橫向V值。

關鍵詞：危險樹木評估、斷層影像、應力波、樹木風險評估、木材密度圖譜。

黃裕星、鍾智昕、吳孟玲、林振榮。2013。大王椰子的應力波斷層影像及木材密度圖譜檢測之案例報告。台灣林業科學28(3):129-44。

INTRODUCTION

In Taiwan, regular inspection of royal palm trees (*Roystonea regia*) is imperative for maintaining in situ structural safety and ensuring public safety (Lin et al. 2011). Tree risk inspections provide a systematic method of examining trees, assessing defects present, and estimating the degree of risk that trees pose to public safety (Pokorny 1992). Arborists evaluate individual trees, assess their hazard potential, and recommend appropriate actions for tree hazard management. The current literature contains methods of decay detection in standing trees, risk assessment guidelines for defective trees, and tree hazard evaluation forms (Matheny and Clark 1994, Harris et al. 2004, Lilly 2010).

Most experts agree that 30~35% of sound wood in the remaining wall (shell) is a

threshold that requires action to be taken; and there are guidelines on the minimum thickness of sound wood (shell) surrounding decaying trunks with and without cavity openings to ensure safety (Hayes 2007). However, criteria that apply to hardwood and softwood trees may be not applicable to royal palms due to differences in their structure and function.

Different acoustic nondestructive evaluations (NDEs) were proven to be effective in detecting and estimating deterioration in tree trunks (Mattheck and Bethge 1993, Bethge et al. 1996, Yamamoto et al. 1998, Divos and Szalai 2002, Pellerin and Ross 2002, Lin et al. 2008, 2011). However, drawbacks of these methods are that the correlation between non-destructive and destructive parameters may

be weak and may be affected by other factors. Moreover, NDE methods cannot be used for direct strength measurements. Therefore, the drawback of NDEs is the relatively inaccurate information generated from strength properties (Kasal 2003). Wood density (D) is an important indicator of strength and is generally regarded as the most important property of a wood. Owing to its strong relationships with other strength properties, D is often the parameter assessed in wood evaluations. The acoustic wave method is a useful inspection technique for estimating the physical strength properties of wood-based timbers. However, when applied to living trees, the acoustic velocity is significantly affected by the moisture content (MC) of the wood. Many researchers have determined that the velocity of an acoustic wave varies with the MC of the wood (Sandoz 1993, Bucur 1995, Wang et al. 2002, 2003, Chan 2007). The velocity of an acoustic wave increases linearly from about saturation to the fiber saturation point (FSP) in longitudinal specimens; it is almost constant in radial specimens; and it decreases linearly in tangential specimens (Wang et al. 2002). However, the effects of different MCs on the transverse stress wave velocity (V) above the FSP in living royal palm trees remain unknown.

In this study, we investigated V tomographies and D profiles in a royal palm tree trunk at different heights. Moreover, the effects of the MC on V during desorption from high MC (270%) to low MC (60%) conditions were examined. The operator must first determine the standardized function between V and MC that should be expected for undamaged wood for a given tree species. Results obtained in this study can facilitate the application of acoustic investigation equipment to risk assessment of royal palm trees to help ensure public safety.

MATERIALS AND METHODS

The purpose of this study was to explore transverse V 2-dimensional (2D) images and D profiles of a royal palm tree trunk at different heights, and the effects of different MCs on the transverse V during desorption. A royal palm tree of 25~30 yr old was selected and felled on March 20, 2012. Then, ten 8-cm-thick undamaged discs were cut from its trunk at 0, 1, 2, 3, 4, 5, 6, 7, 8, and 9 m above ground level for V 2D imaging and D profile experiments. Another 4 undamaged discs of the same thickness were randomly cut from the trunk at different heights above the ground level to explore effects of different MCs on the transverse V. All 14 discs were immediately transported to the Taiwan Forestry Research Institute in Taipei, Taiwan for further investigation.

Acoustic 2D tomography was conducted using a Fakopp 2D Microsecond Timer (Fakopp Enterprise, Agfalva, Hungary). Multiple stress-wave measurements (8 probes) were made on the first 10 discs at 8 equidistant points. Sensors were installed on the discs, and a transducer was connected at an angle of 90° to the trunk axis to detect the propagating stress wave velocity. Measurements were repeated for all other positions of the transmitter probe, allowing for 28 (for a full round trip; 7 receiving probes x 8 transmitter probes ÷ 2 same paths) independent propagation time measurements for each investigated section. A complete data matrix was obtained through this measurement process for each test disc (Fig. 1).

The weight of the disc was measured immediately after the stress wave inspection. The green MC was calculated using the following formula:

$$MC (\%) = [(W_g - W_o) / W_o] \times 100; \quad (1)$$

where W_g is the green weight (g) and W_o is

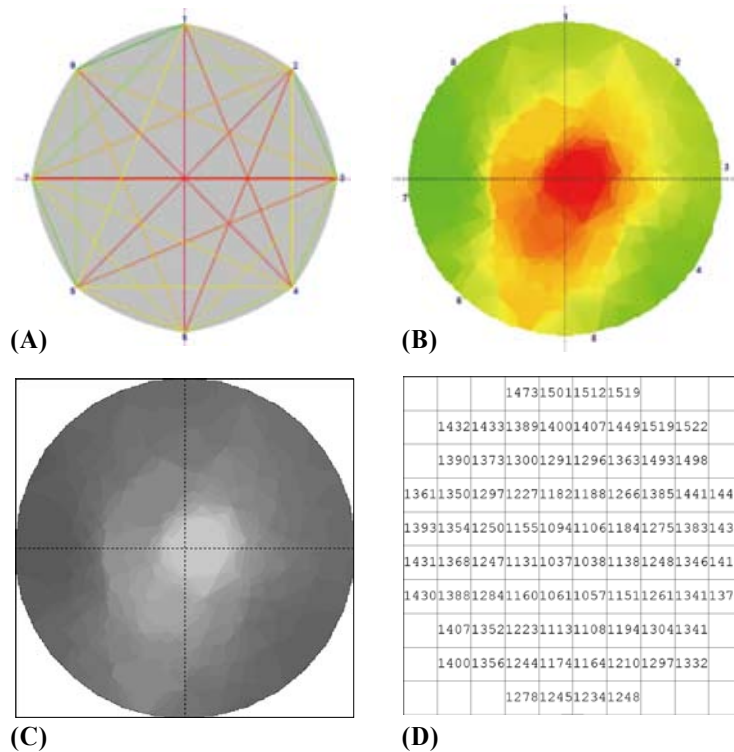


Fig. 1. Sensor arrangement, path of transverse stress wave measurements, and 2D tomogram of the experimental procedure (from A to D).

(A) Acoustic image test using multi-channel stress wave (8 probes).

(B) Constructed 2D image (yellow-green-red).

(C) Conversion of the 2D image (B) into 256 gray shades.

(D) Corresponding transverse acoustic velocity calculated for every grid square.

the oven-dry weight (g).

A diametrical strip about 20 mm wide (from the dense peripheral region to the less-dense inner region of the tree trunk) was sawn from each disk in the same direction (east-west). A thin slice (2 × 20 mm, virtual longitudinal × tangential) for x-ray scanning was cut from each strip (Fig. 2). All sampled strips were conditioned at an MC of 12% to calculate the wood D profile.

D profiles of the conditioned slices were determined using a direct-reading x-ray densitometer (QTRS-01X Tree Ring Analyzer; Quintek Measurement Systems (QMS), Knoxville, TN, USA). The determination

of density was based on the relationship of x-ray attenuation and density (QMS 1999). Specimens were conditioned in a controlled environment room at 20°C and 65% relative humidity (D profile at about an MC of 12%). Each slice was scanned and moved through the x-ray machine in the radial direction. A standard collimator supplied with the tree ring analyzer yielded an approximate width of 0.038 mm and a height of 1.59 mm at the detector. The sample step size could be adjusted at 0.02-mm increments. With the QTRS-01X scanning system, the wood density can be determined according to the x-ray attenuation. A positive relationship exists between the wood

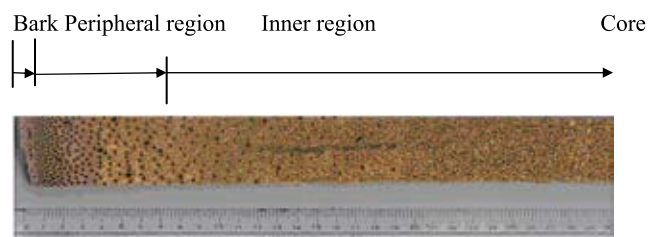


Fig. 2. X-ray scanning specimen in the radial direction.

density and x-ray attenuation; that is, the higher the wood density, the larger the x-ray attenuation, and vice versa (QMS 1999).

To study the effects of the MC on V during desorption, the remaining 4 undamaged discs cut randomly at different heights were first immersed in water for more than 3 wk until they reached a near-saturation MC of 270%. Then, they were removed for acoustic 2D tomographic inspection using the stress wave method described above. In brief, a stress wave was propagated through the disc, and MC levels at which weight loss of about 100~200 g occurred were recorded until the MC reached 60%. The MC was calculated using formula (1).

For each disc, the circumference and distances between sensors were obtained using a tape measure. The measurements served as inputs to the system software to map the approximate geometric form of the cross-sections. With the acoustic measurements obtained, a tomogram (2D image) was constructed for each cross-section using Fakopp ArborSonic software. To quantitatively assess the tomograms, all corresponding stress wave velocity values at each pixel were further calculated by visualizing and converting the tomogram (Fig. 1), and stress wave velocity maps of the cross-sections were obtained for further analysis.

In this study, a cross-section in the radial position was divided by visual observation into 2 regions according to obvious vascular

bundles and color change (actual position for comparing the wood density profile), namely, a dense peripheral region (from the bark inward to about 25~50 mm distance from bark) and a less-dense inner region (from about 25~50 mm distance from bark to the inner trunk region), as shown in Fig. 3.

The 2D image was built according to transverse V values of different detection paths. Moreover, all corresponding V values at each pixel were further calculated by image analysis, and a V grip map of the cross-sections was obtained for the V profile according to the smoothing spline method. The correlation coefficient (R^2 , determination coefficient) of the relationship between factors x



Fig. 3. Cross-section of a royal palm tree trunk.

and y was calculated by a Pearson correlation analysis (at a significance level of $\alpha = 0.05$).

RESULTS

Trunk diameter and green MC

Figure 4 shows variations in the trunk diameter and MC at different tree heights. As can be seen, the trunk diameter first decreased from ground level (0 m) to a minimum of 30 cm at 2 m, increased thereafter to a maximum of 41.5 cm at 6 m above ground, and then declined again. With such inconsistent fluctuations, the palm trunk was neither cylindrical nor tapering toward the tree top.

As for the MC, a significant drop was observed from a maximum of 208.7% at ground level to a minimum of 67.0% at 2 m above ground. Thereafter, the MC rose significantly to 185.3% at 3 m above ground, followed by fluctuations of a smaller magnitude. The average MC of 10 discs in the palm tree was 165.4%.

Variations in V and D from the bark to the core

Figure 5 shows corresponding 2D images of the transverse V at different tree

heights. As can be seen, at all tree heights, the peripheral region showed a larger V than the inner region. The same trend can be seen in Fig. 6, in which the bold line (pink) indicates variations in the V with increasing distance from the bark. All bold lines revealed an increase in the V in the peripheral region, reaching its maximum around 25 mm from the bark, followed by a decrease in the V with increasing distance towards the inner region. At the same time, the V tended to be larger in the peripheral region of higher wood density but smaller in the inner region of lower wood density. The same findings can be seen in Fig. 7, which shows variations in average V and D values at different tree heights with increasing distance from the bark to the core. As can be seen, the largest V was observed in the peripheral region at about a 10~15-mm distance from the bark, while the smallest V was found in the inner region near the trunk core. Similar changes in the D profile from the bark to the core were observed. As can be seen in Fig. 7, the D increased sharply from the bark inward and peaked at around a 5~10 mm-distance from the bark. It then decreased gradually at 25~60 mm from the bark and remained more or less the same thereafter with

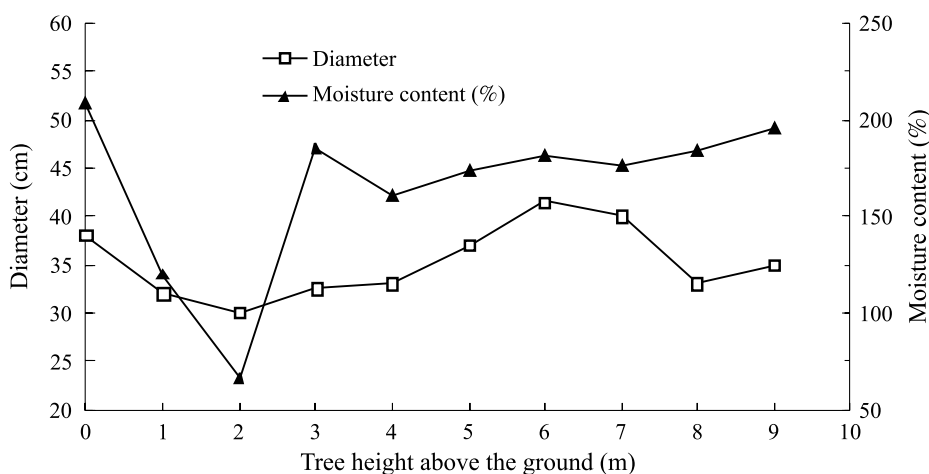


Fig. 4. Trunk diameter and moisture content at different tree heights.

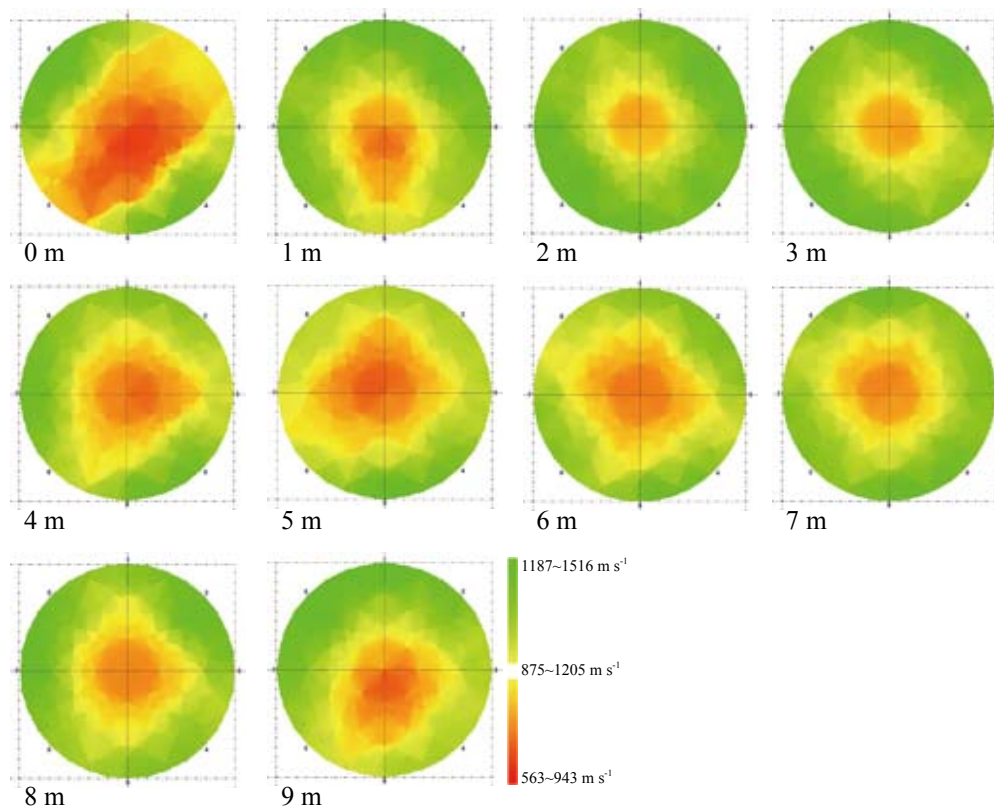


Fig. 5. 2D images of transverse stress wave velocities obtained at different tree heights.

increasing distance toward the core. In other words, the peripheral region of the disc was denser than its inner region. The above results and observations reveal that the average thickness of peripheral wood was in general about 25~50 mm at various heights.

Variations in V and D values with tree height

Figure 8 shows variations in V and D values at different tree heights. As can be seen, the transverse V first increased from the ground level, reached an average maximum of 1324.7 m s^{-1} at 2 m above the ground, then dropped gradually to an average minimum of 842.6 m s^{-1} at 5 m above the ground, and finally rose again. A similar trend of changes in the D at different tree heights was observed.

As shown in Fig. 8, D first increased from the ground level, reached a maximum of 464.6 kg m^{-3} at 2 m above the ground, then dropped gradually to a minimum of 242.2 kg m^{-3} at 6 m above the ground, and finally rose again.

Figure 9 shows average V and D value in the peripheral (PV and PD) and inner regions (IV and ID). Both PV and IV exhibited the same trend. They first increased from the ground level, peaked respectively at 1 and 2 m above the ground, dropped to their lowest at 5 m above the ground, and then rose again. Changes in PD and ID values were less marked but had a similar trend. They first increased from the ground level, peaked at 2 m above the ground, dropped to their lowest at 6 m above the ground, and then rose again.

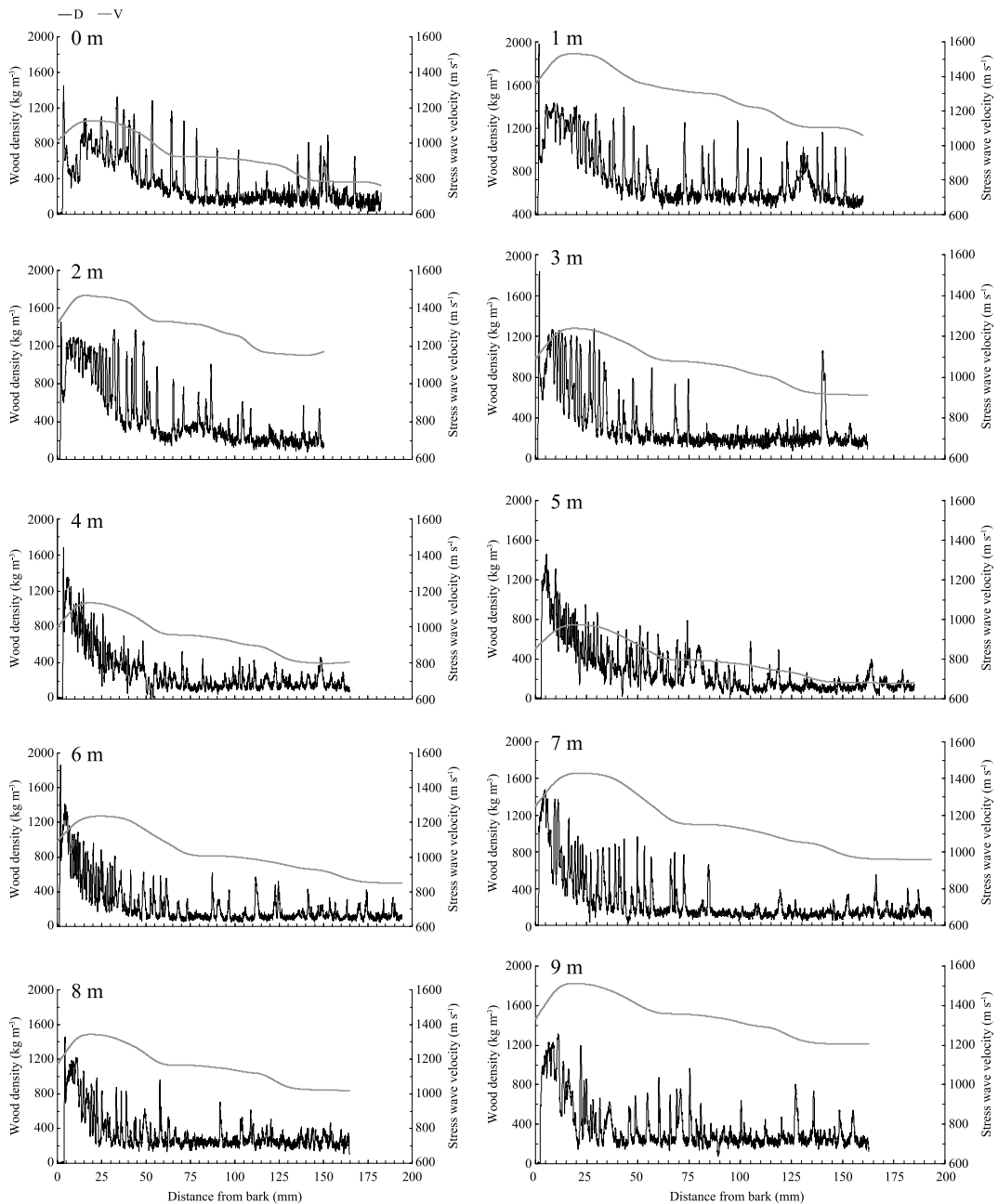


Fig. 6. Variations in the transverse stress wave velocity (V) by smoothing spline and wood density profiles (D) at different tree heights. V: gray solid line; D: black solid line.

Thickness and ratio of periphery wood

Figure 10 shows variations in the thickness and ratio of the peripheral region at different tree heights. The thickness was deter-

mined by visual observation, while the ratio was calculated by dividing the thickness by the diameter. As can be seen, an inverse relationship existed between the thickness of the

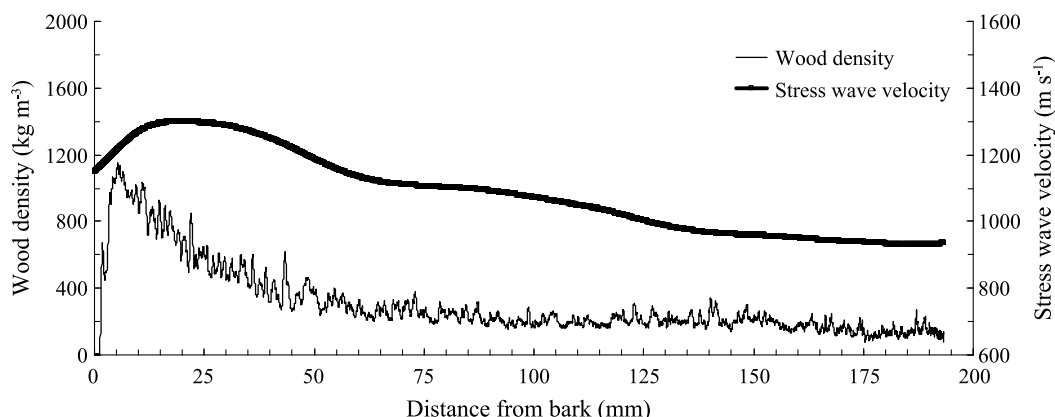


Fig. 7. Variations in average transverse stress wave velocity (V) and average wood density profiles (D) based on different tree heights from the bark to the core.

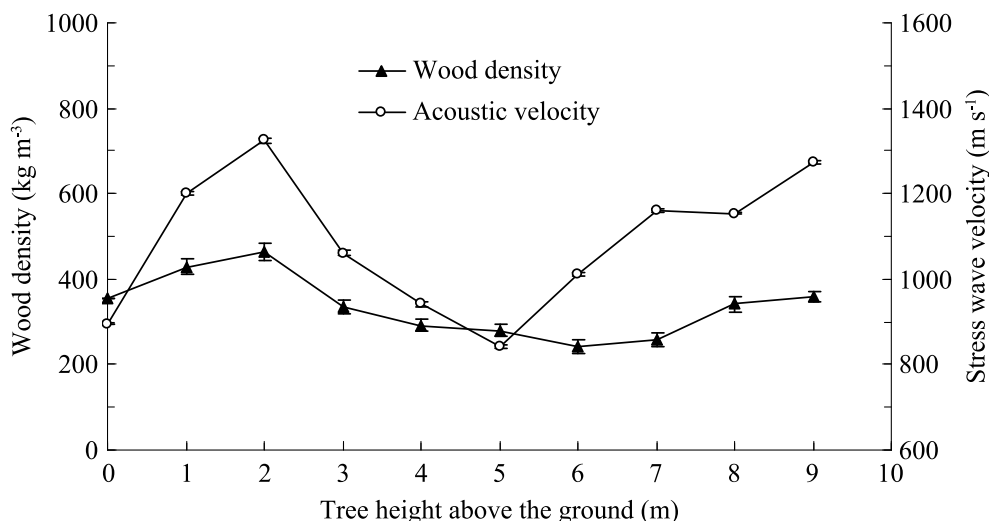


Fig. 8. Variations in average transverse stress wave velocity (V) and wood density profiles (D) at different tree heights. (I, standard error).

peripheral region and tree height; that is, the thickness of the peripheral region decreased with increasing tree height. As can be seen in Fig. 10, the peripheral region was thickest (6 cm) at ground level. The decrease was steady with more-marked drops in thickness at 0~1 and 5~6 m above the ground. A similar declining tendency was observed for the ratio of the peripheral region with increasing tree height. That is, the ratio of the peripheral region was at a maximum of 15.8% at ground

level, then fluctuated at different tree heights, reached a minimum of 6% at 6 m above the ground, and then increased again. In summary, both the thickness and ratio of the peripheral region peaked at the tree base.

Relationships of the D with V and of MC with V

Figure 11 shows the relationship between the D (at about 12% MC) and V (green, on March 20, 2012). The relationship can be

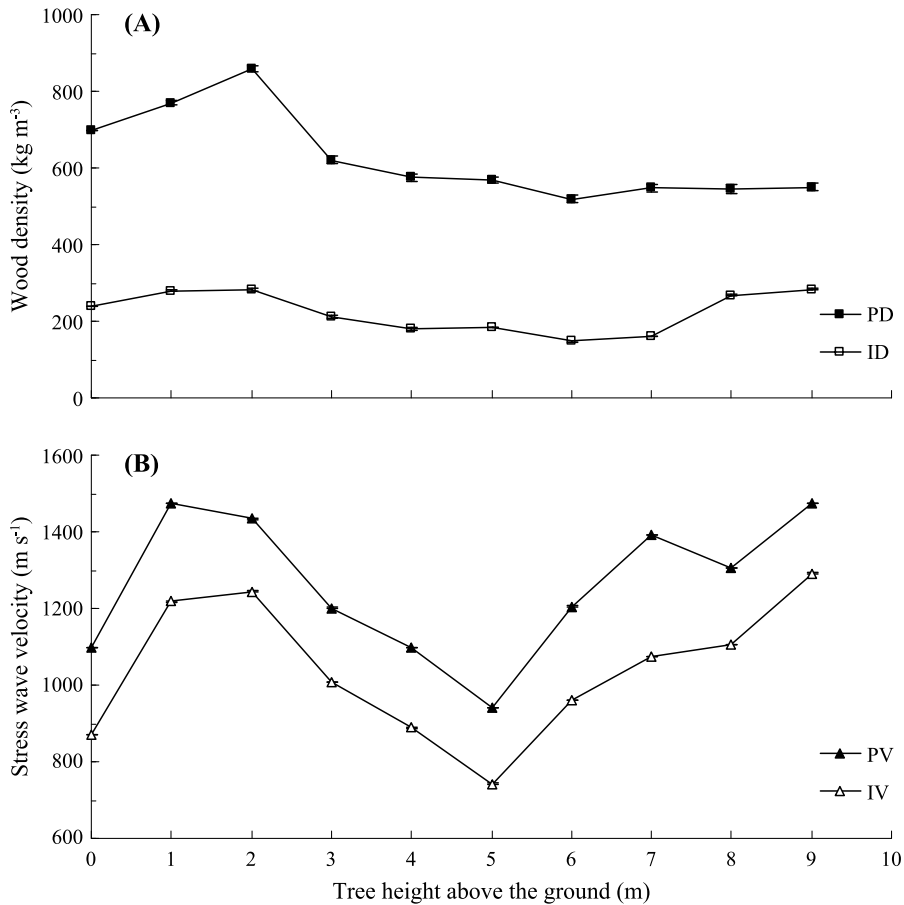


Fig. 9. Transverse stress wave velocities and wood densities of (A) the peripheral (PV and ID) and (B) inner regions (PV and IV) at different tree heights (I, standard error).

expressed by a second-order polynomial regression, and the model was highly significant (the coefficient of determination, $R^2 = 0.82$, $p < 0.01$). As can be seen, the distribution of higher ($> 700 \text{ kg m}^{-3}$) and lower ($< 300 \text{ kg m}^{-3}$) D values had lower levels as predicted by the V, indicating a large discrepancy and high inaccuracy.

Figure 12 shows the relationship between the MC and V. As can be seen, a linear relationship existed between the two; that is, the higher the MC was, the larger the V was. In this study, the transverse V of each disc was adjusted to a single MC of 165.4% (average value in living trees) according to analyti-

cal results of Fig. 12. Figure 13 shows the relationship between the adjusted V (at 165.4% MC) and D (at about 12% MC). Similarly, a linear relationship existed between the two; that is, the higher the V was, the larger the D was. When expressed as a linear regression relationship, R^2 was 0.54 ($p < 0.01$).

DISCUSSION

There are some predictions for possible causes of longitudinal and transverse MC variations depending on the literature (Zobel and van Buijtenen 1989, Tomlinson 1990). However, there is no satisfactory knowledge

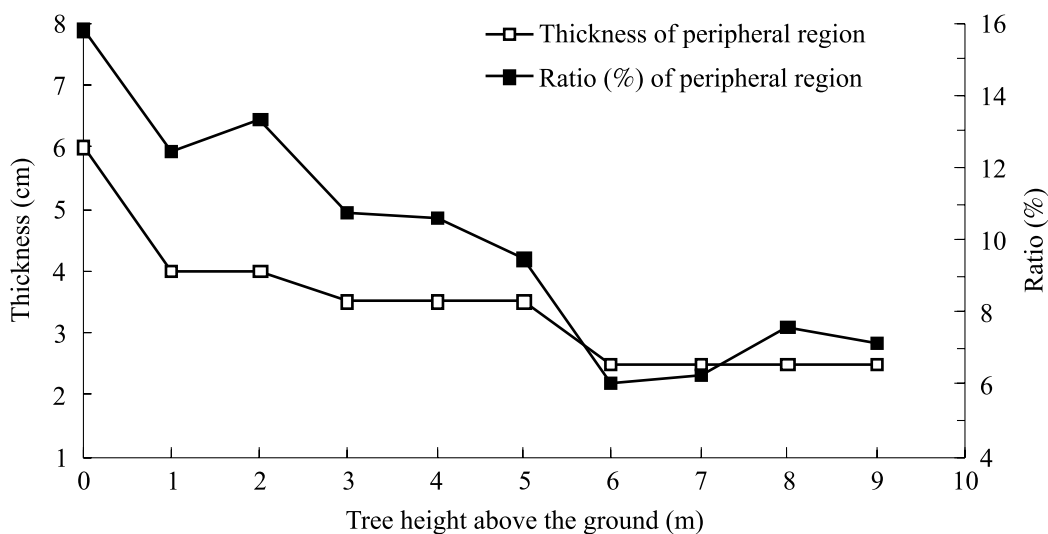


Fig. 10. Variations in the thickness and ratio of the peripheral region at different tree heights.

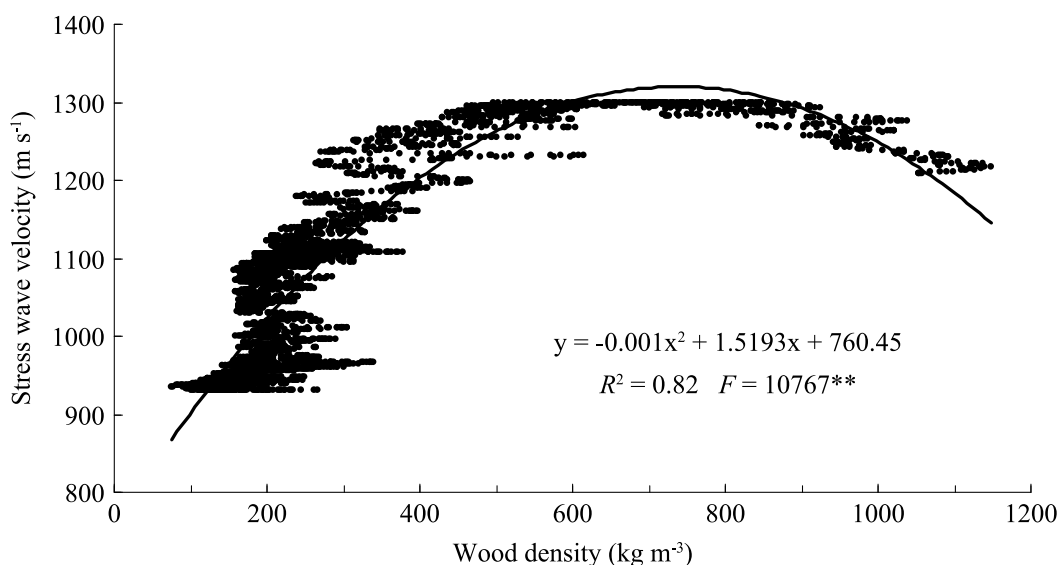


Fig. 11. Relationship between the wood density (at about a 12% moisture content) and stress wave velocity of a living tree.

or explanation for the actual situation. In this study, the palm trunk was neither cylindrical nor tapering toward the tree top. In general, the growth in trunk diameter is influenced by annual weather conditions including temperature and precipitation. As for the MC in this study, a significant drop was observed from

a maximum of 208.7% at ground level to a minimum of 67.0% at 2 m above the ground. According to Chiu and Lin (2007), there can be considerable MC variations in trees depending on the season, soil MC, and age and growth of the tree. In addition, too-high or too-low MCs would imply physiological

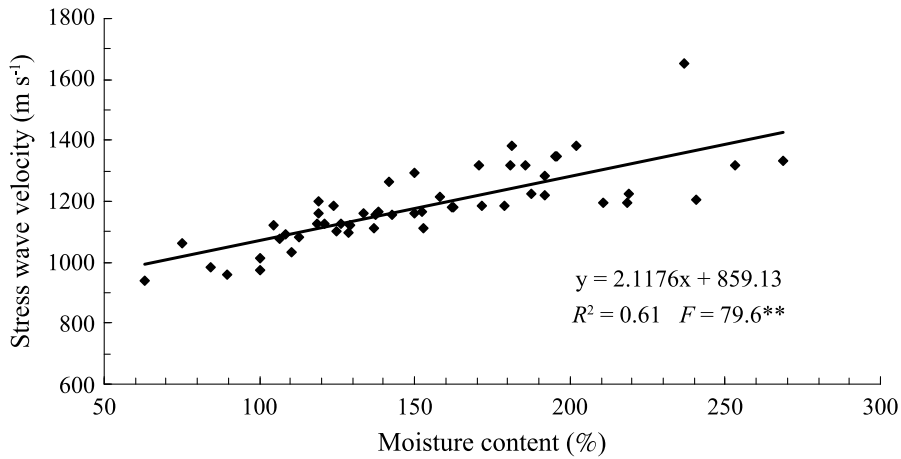


Fig. 12. Relationship between the moisture content and stress wave velocity.

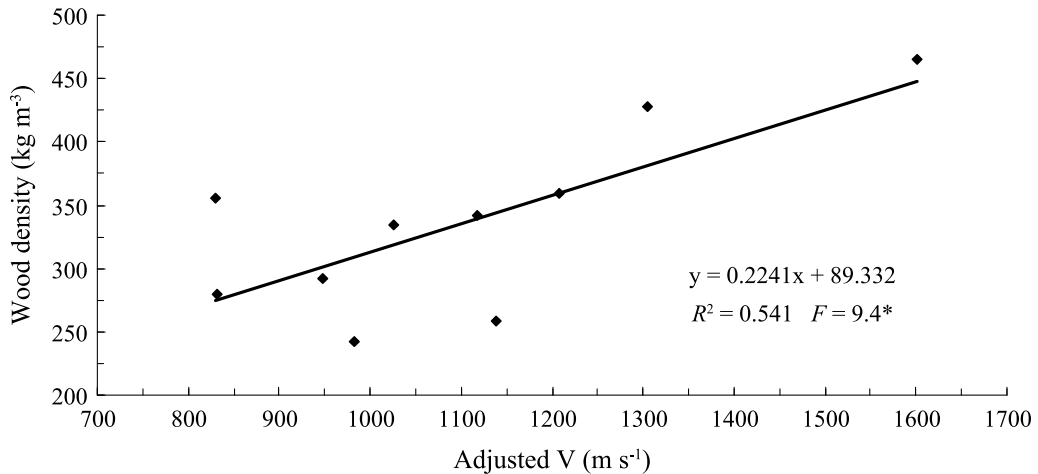


Fig. 13. Relationship between the wood density (at about a 12% moisture content) and adjusted stress wave velocity (V , at a moisture content of ~165.4%).

problems of the tree, which merit attention.

Rich (1987) and Tomlinson (1990) reported that the highest D of palm trunks is located in the peripheral region. Consistent with their findings, our results observed an increase in the D inward from the bark, which remained high to around 25–50 mm from the bark, followed by a gradual decline toward the trunk core. Mattheck and Breloer (2003) indicated that the most important and most dangerous load on the tree is undoubtedly that created by wind, which can introduce bend-

ing stresses near the periphery of the trunk. de Castro et al. (1993) reported that with successive increases in trunk diameter, new secondary xylem with higher wood density is produced to compensate for structural weaknesses, and radial increases in D are normal.

The D profiles in Fig. 6 show many spikes, indicating abrupt raised peaks of high D in the tree trunk, which can be attributed to the presence of vascular bundles detected by x-ray scanning. As seen in Figs. 2 and 3, the density of vascular bundles significantly de-

creased from the peripheral region to the inner region in the direction of the core. Harris et al. (2004) indicated that fibers that support palm trunks occur in discontinuous bundles, and palms lack secondary xylem that forms annual rings of wood found in typical trees. Moreover, patterns of decay development and compartmentalization found in trees are also absent from palms. In Tomlinson's (1990) anatomy of individual vascular bundles, metaxylem, metaploem, and fibrous bundle sheaths, as shown in Fig. 14, were present in the tree trunk. Apart from providing support, vascular bundles also serve physiological functions of transporting water and nutrition to different parts of the tree.

As seen in Fig. 5, the corresponding radial *V* values of undamaged disc cross-sections from the peripheral region (outer layer, higher *D*) to the inner region (inner layer, lower *D*) showed a symmetrical layered structure (*D* and *V* profiles in cross-section). On the contrary, a non-symmetrical layered structure is indicative of unsound trunk problems. For more in-depth inspection of acoustic equipment, the color scale of *V* has to be adjusted

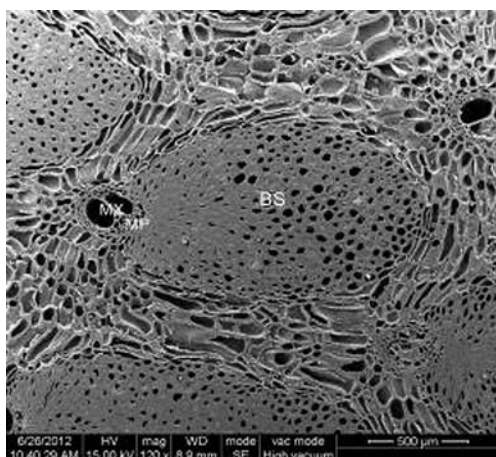


Fig. 14. Anatomic structures in a disc cross-section. BS, fibrous bundle sheath; MX, metaxylem; MP, metaploem.

to determine the exact location and extent of a defect; moreover, the accuracy and reliability of tomograms in palm trees should be confirmed by another NDE tool. This approach was previously adopted by Lin et al. (2011) in their investigation of the wood quality of standing royal palms in the peripheral and inner regions (2D) first using ultrasonic velocity tomography, followed by resistance micro-drilling techniques to locate the position and area of the defects.

Both Rich (1987) and Tomlinson (1990) reported that the maximum *D* in palm trunks is located close to the tree base. Our observations are consistent with their findings. In the study, the highest *D* and *V* values were found in the peripheral region of the trunk at 1~2 m above the ground, while the lowest *D* and *V* values were observed in the inner region of the trunk at 5~6 m above the ground. This has significant implications for the resistance of palm trees against the wind. In a strong wind, tree base and tree top are the most vulnerable. Hence, a sturdy structure is required to resist against forces generated by the wind. Variations in the *D* and *V* in the trunk at different heights reflect the distribution of strength required to overcome the forces of a strong wind.

In the literature, Zobel and van Buijtenen (1989) came up with 4 general categories of wood classified according to changes in the *D* from the base to the top of a tree. They include type I with *D* decreasing from the base to the top, type II with *D* increasing from the base to the top, type III with *D* decreasing for some distance up the tree, followed by an increase toward the top, and type IV with no variations in *D* at different heights. While there is no prior research examining to which category palm trees belong, our results showed that they seem to fit in type III except for the initial increase in *D* from the base to about 2 m above the ground.

A larger thickness of the peripheral region and a higher ratio of peripheral wood toward the trunk base have significant implications for the tree structure and safety. In this study, ratios of peripheral wood at different tree heights ranged 6~15.8%. Most experts (Pokorny 1992, Matheny and Clark 1994, Harris et al. 2004, Hayes 2007) agreed that a ratio of 30~35% of sound wood in the remaining wall is the threshold that requires some action to be taken. Generally, larger-crown trees need to produce greater support; however, the smaller crown of palm trees (trunk) needs to withstand smaller forces. Therefore, ratios of peripheral wood of palm trees are smaller compared to those of general trees (softwoods and hardwoods) for supporting the living tree body. The ratio of sound wood is calculated using the following formula: (width of sound wood/radius of the trunk) \times 100%. A ratio of 15% of sound wood surrounding (thickness) decaying columns (diameter) in the trunk would imply high risk, and a ratio of 10% represents a critical risk. Another important tree safety index is the ratio of the cavity opening to the circumference, calculated using the following formula: (width of the cavity opening/circumference) \times 100%. A ratio exceeding 40% would indicate a high risk posed to public safety.

Previous research reported significant impacts of MCs of wood on the V (Sandoz 1993, Bucur 1995, Wang et al. 2002, 2003, Chan 2007). Our findings provide further evidence supporting the influence of water in the palm disc on the measured V and the tendency of the V to increase with the MC. Wang et al. (2002) pointed out that the V increased linearly from saturation to the FSP in longitudinal specimens, remained almost constant in radial specimens, but decreased linearly in tangential specimens. Owing to differences in vascular anatomy, palm trees show simi-

lar V and wood properties in the tangential direction, but not in the radial direction. As mentioned above, the acoustic velocity was affected by different MCs in standing trees. Hence, adjustment of the V for the same MC status would enhance the accuracy of stress wave inspection and facilitate comparisons of wood properties in standing trees.

CONCLUSIONS

This study examined transverse V tomograms and wood-density profiles of a royal palm tree trunk at different heights. Moreover, the effects of the different MCs of 60~270% on the transverse V during desorption were investigated, with the following results.

1. As to variations in the MC at different tree heights, a significant drop was observed from a maximum of 208.7% at ground level to a minimum of 67.0% at 2 m above the ground. The average MC of 10 discs in a palm tree was 165.4%.
2. Corresponding radial V and D values of an undamaged disc cross-section from the peripheral region (higher) to the inner region (lower) showed a symmetrical layered structure. The peripheral region of the disc was denser than its inner region. The average thickness of peripheral wood was in general about 25~50 mm at various heights.
3. The average highest V and D values on the tree trunk were both located at 2 m above the ground, while the average lowest V and D values on the tree trunk were found at 5~6 m above the ground.
4. Visual inspection of disc cross-section revealed a larger thickness and ratio in the peripheral region of the tree trunk at the tree base.
5. The relationship between the D (at about a 12% MC) and V (green) can be expressed by a second-order polynomial regression (R^2

= 0.82, $p < 0.01$).

6. The V was significantly ($R^2 = 0.61$, $p < 0.01$) affected by the MC and tended to increase with an increasing MC. When making an acoustic inspection, it is necessary to adjust the V of standing trees with different MCs for comparison purposes and to achieve higher accuracy, which would in turn yield more-accurate tree inspection assessments.

ACKNOWLEDGEMENTS

The authors thank Ms. Jin-Mei Lee for her assistance with the photography (fibrous bundle sheath of Fig. 14).

LITERATURE CITED

- Bethge K, Mattheck C, Hunger E. 1996.** Equipment for detection and evaluation of incipient decay in trees. *Arboric J* 20:13-37.
- Bucur V. 1995.** Acoustics of wood. Boca Raton, FL: CRC Press. p 77-201.
- Chan JM. 2007.** Moisture content in radiata pine wood: implications for wood quality and water-stress response. Phd thesis, School of Forestry, College of Engineering, Univ. of Canterbury, Christchurch, NZ. p 202.
- Chiu CM, Lin CJ. 2007.** Radial distribution patterns of the green moisture content in trunks of 46-year-old red cypress (*Chamaecyparis formosensis*). *J Wood Sci* 53:374-80.
- de Castro F, Williamson GB, de Jesus RM. 1993.** Radial variation in the wood specific gravity of *Joannesia princeps*: the roles of age and diameter. *Isotopic* 25:176-82.
- Divos F, Szalai L. 2002.** Tree evaluation by acoustic tomography. Proceedings of the 13th International Symposium on Nondestructive Testing of Wood. August 19-21, 2002. Berkeley, CA: Univ. of California, Berkeley Campus. p 251-6.
- Harris RW, Clark JR, Matheny NP. 2004.** Arboriculture: integrated management of landscape trees, shrubs, and vines. Upper Saddle River, NJ: Pearson Education. p 405-33.
- Hayes E. 2007.** Evaluating tree defects, a field guide. Rochester, MN: Safetrees LLC. p 30.
- Kasal B. 2003.** Semi-destructive method for in-situ evaluation of compressive strength of wood structural members. *For Prod J* 53(11/12):55-8.
- Lilly SJ. 2010.** Arborists' certification study guide. Champaign, IL: International Society of Arboriculture. p 198-213.
- Lin CJ, Chang TT, Juan MY, Lin TT. 2011.** Detecting deterioration in royal palm (*Roystonea regia*) using ultrasonic tomographic and resistance microdrilling techniques. *J Trop For Sci* 23:260-70.
- Lin CJ, Kao YC, Lin TT, Tsai MJ, Wang SY, Lin LD, et al. 2008.** Application of an ultrasonic tomographic technique for detecting defects in standing trees. *Int Biodeter Biodegr* 43:237-9.
- Matheny NP, Clark JR. 1994.** A photographic guide to the evaluation of hazard trees in urban areas. Champaign, IL: International Society of Arboriculture. p 85.
- Mattheck C, Breloer H. 2003.** The body language of trees: a handbook for failure analysis. London: HMSO Publications. 240 p.
- Mattheck CG, Bethge KA. 1993.** Detection of decay in trees with the Metriguard Stress Wave Timer. *J Arboric* 19:374-8.
- Pellerin RF, Ross RJ. 2002.** Nondestructive evaluation of wood. Madison, WI: Forest Products Society, USA. p 149-56.
- Pokorny JD. 1992.** Urban tree risk management: a community guide to program design and implementation. Washington, DC: USDA Forest Service Northeastern Area State and Private Forestry. p 194.
- QMS. 1999.** QMS Tree Ring Analyzer Users Guide Model QTRS-01X. Knoxville, TN: Quintek Measurement Systems (QMS). p 53.

- Rich PM. 1987.** Mechanical structure of the stem of arborescent palms. *Bot Gaz* 148(1):42-50.
- Sandoz JL. 1993.** Moisture content and temperature effect on ultrasound timber grading. *Wood Sci Technol* 27:373-80.
- Tomlinson PB. 1990.** The structural biology of palms. Oxford, NY: Clarendon Press. p 123-30, 165-9.
- Wang SY, Chiu CM, CJ Lin. 2002.** Variations in ultrasonic wave velocity and dynamic Young's modulus with moisture content for *Taiwania* plantation lumber. *Wood Fiber Sci* 34:370-81.
- Wang SY, Lin CJ, Chiu CM. 2003.** The adjusted dynamic modulus of elasticity above the fiber saturation point in *Taiwania* plantation wood by ultrasonic-wave measurement. *Holzforchung* 57:547-52.
- Yamamoto K, Sulaiman O, Hashim R. 1998.** Nondestructive detection of heart rot on *Acacia mangium* trees in Malaysia. *For Prod J* 48:83-6.
- Zobel BJ, van Buijtenen JP. 1989.** Wood variation: its causes and control. Berlin: Springer-Verlag. p 218-48.